Available online at www.sciencedirect.com
ScienceDirect
Journal of Solid State Chemistry 180 (2007) 1158–1162
JOURNAL OF SOLID STATE CHEMISTRY
www.elsevier.com/locate/jssc

Rapid communication

Thermoelectric properties of Ag-doped n-type $(Bi_2Te_3)_{0.9}$–$(Bi_{2-x}Ag_xSe_3)_{0.1}$ ($x = 0$–0.4) alloys prepared by spark plasma sintering

J.L. Cui[a,*], W.J. Xiu[a,b], L.D. Mao[a,c], P.Z. Ying[b], L. Jiang[b], X. Qian[c]

[a]*School of Mechanical Engineering, Ningbo University of Technology, Ningbo 315016, China*
[b]*School of Materials Science and Engineering, China University of Mining and Technology, Xuzhou 221008, China*
[c]*College of Chemical Engineering and Materials Science, Zhejiang University of Technology, Hangzhou 310014, China*

Received 5 October 2006; received in revised form 2 December 2006; accepted 11 December 2006
Available online 15 December 2006

Abstract

Ag-doped n-type $(Bi_2Te_3)_{0.9}$–$(Bi_{2-x}Ag_xSe_3)_{0.1}$ ($x = 0$–0.4) alloys were prepared by spark plasma sintering and their physical properties evaluated. When at low Ag content ($x = 0.05$), the temperature dependence of the lattice thermal conductivity follows the trend of $(Bi_2Te_3)_{0.9}$–$(Bi_2Se_3)_{0.1}$; while at higher Ag content, a relatively rapid reduction above 400 K can be observed due possibly to the enhancement of scattering of phonons by the increased defects. The Seebeck coefficient increases with Ag content, with some loss of electrical conductivity, but the maximum dimensionless figure of merit ZT can be obtained to be 0.86 for the alloy with $x = 0.4$ at 505 K, about 0.2 higher than that of the alloy $(Bi_2Te_3)_{0.9}$–$(Bi_2Se_3)_{0.1}$ without Ag-doping.

Keywords: Thermoelectric property; Spark plasma sintering; n-type pseudo-binary $(Bi_2Te_3)_{0.9}$–$(Bi_{2-x}Ag_xSe_3)_{0.1}$ alloys

1. Introduction

Narrow gap semiconductors Bi_2Te_3 and Bi_2Se_3 are classic room temperature thermoelectric materials. In spite of a long history of research, there is an ongoing effort toward the improvement of thermoelectric properties of Bi_2Te_3, Bi_2Se_3 and their related alloys [1,2]. Strategies to further improve the figure of merit (ZT) of these two semiconductors generally involve decreasing the lattice thermal conductivity through a number of techniques that affect the microstructure of the material. These include solid-solution alloying of these two and other different semiconductors [3,4], an increase of concentration of Bi_2Se_3 in the $Bi_2(Te_{1-x}Se_x)_3$ [5] and dispersing inert particles in the semiconductors [6]. The above treatments can all disrupt the regular ordering of the crystalline grains and decrease the ability of the material to carry heat through lattice vibrations.

The crystal structure of $(Bi_2Te_3)_{0.9}$–$(Bi_2Se_3)_{0.1}$ is rhombohedral with space group $D^5_{3d}(R\bar{3}m)$ [7], since at temperature above 500 °C Bi_2Te_3 and Bi_2Se_3 can form a continuous solid solution [8]. For Bi_2Se_3 and Bi_2Te_3 it can be represented as a stack of hexagonally arranged atomic planes, each consisting of only one type of atom. Five atomic planes are stacked in a close-packed fcc fashion in order Te1(Se1)–Bi–Te2(Se2)–Bi–Te1(Se1), in a quintuple layer. The stoichiometric as-grown Bi_2Se_3 samples are n-type with carrier concentration of about 10^{19} cm^3, doping samples with excess Bi introduces substitutional Bi defects at the Se sites (Bi_{Se} antisites), which are shallow acceptors [9]. Recent works [10–12] evidenced that different Ag concentrations doped in p-type Bi–Sb–Te alloys reveal a significant enhancement of electrical conductivities and reduction of thermal conductivities, leading to the improvement of figure of merit ZT. While in n-type Bi–Se related alloys, if element Ag substitutes for Bi in the Bi_2Se_3, it can be assumed that the $(Bi_2Te_3)_{0.9}$–$(Bi_{2-x}Ag_xSe_3)_{0.1}$ is still be n-type semiconductor due to an interstitial donor action of the elemental Ag possibly resided in the van der

*Corresponding author. Fax: +86 574 8708 1258.
E-mail address: cuijl@nbip.net (J.L. Cui).

0022-4596/$ - see front matter © 2006 Elsevier Inc. All rights reserved.
doi:10.1016/j.jssc.2006.12.010

Walls planes. As this treatment could also disrupt the regular ordering of the crystalline of $(Bi_2Te_3)_{0.9}$–$(Bi_{2-x}Ag_xSe_3)_{0.1}$, the possible reduction can be expected of both the lattice and electronic thermal conductivities without noticeable loss of the electrical conductivity.

In the present work, Ag-doped pseudo-binary $(Bi_2Te_3)_{0.9}$–$(Bi_{2-x}Ag_xSe_3)_{0.1}$ ($x = 0$–0.4) alloys were prepared by spark plasma sintering, and the effect of Ag concentration on their thermoelectric properties evaluated.

2. Experimental

Two mixtures, consisting of elements Ag, Bi, Se and Te with a purity of more than 99.999% in stoichiometric ratio of compounds Bi_2Te_3 and $Bi_{2-x}Ag_xSe_3$ ($x = 0$–0.4), were sealed in two different evacuated quartz tubes and then melted for 10 h at 1323 K, during which 30-s rocking every 1 h was conducted to ensure that the composition was homogenous without segregation. After quenching, the two ingots (Bi_2Te_3 and $Bi_{2-x}Ag_xSe_3$) were once more sealed and melted in vacuum tubes according to stoichiometry of $(Bi_2Te_3)_{0.9}$–$(Bi_{2-x}Ag_xSe_3)_{0.1}$ ($x = 0$–0.4). The obtained $(Bi_2Te_3)_{0.9}$–$(Bi_{2-x}Ag_xSe_3)_{0.1}$ ingots with different molar fraction x were ball-milled in stainless steel bowls for 5 h with a rotation rate of 350 rpm. The powders after drying in vacuum for 5 h at 60 °C were sintered at 623 K with a pressure of 40 MPa using a spark plasma sintering apparatus (SPS-1030), and the samples obtained with the size of ϕ 20 mm × 2.5 mm were eventually cut into 3 mm slices measuring 2.5 mm × 15 mm. The densities of the samples were measured using an Archimedes method, and range from 7.68 to 8.05 kg m^{-3}.

The Seebeck coefficients (α) and electrical conductivities (σ) were measured using an apparatus (ULVAC ZEM-2) in a helium atmosphere. Thermal diffusivities were measured by a laser flash method (TC-7000 H), and thermal conductivities were calculated from the values of density, specific heat and thermal diffusivity. The structural analyses were directly taken with X-ray diffractometer (XRD-98) using Cu$K\alpha$ radiation ($\lambda = 0.15406$ nm), using a scan rate of 4° min^{-1} to record the patterns in the 2θ range from 10° to 100°. The chemical compositions were analyzed with Electron Probe Microanalysis (EPMA-8705QH2) with an accuracy of more than ±97%.

3. Results and discussion

Fig. 1 shows the XRD patterns for the synthesized $(Bi_2Te_3)_{0.9}$–$(Bi_{2-x}Ag_xSe_3)_{0.1}$ ($x = 0$–0.4) alloys. It can be observed that the alloys show a typical rhombohedral structure as that of $(Bi_2Te_3)_{0.9}$–$(Bi_2Se_3)_{0.1}$. The addition of Ag element into the Bi–Se alloys could help the formation of Ag–Se bonds at the expense of Bi–Se bonds, since the bonding energy increases roughly with the melting point of materials, according to the Saxane's suggestion [13]. Despite the maximum molar fraction x of 0.4 in the pseudo-binary $(Bi_2Te_3)_{0.9}$–$(Bi_{2-x}Ag_xSe_3)_{0.1}$ alloys, we still

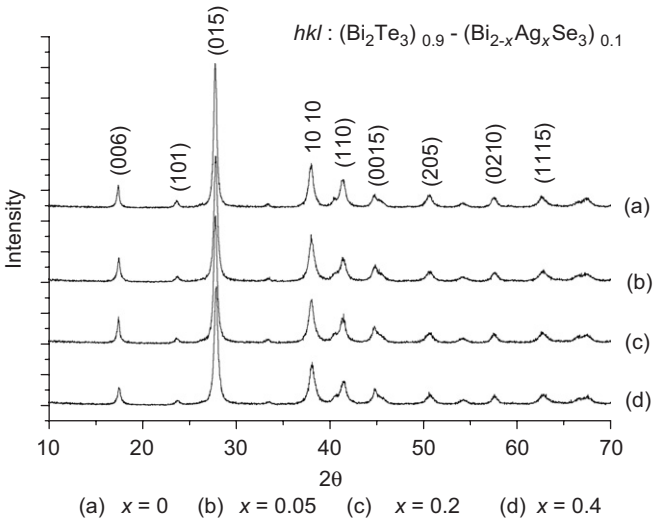

Fig. 1. X-ray diffraction patterns of the $(Bi_2Te_3)_{0.9}$–$(Bi_{2-x}Ag_xSe_3)_{0.1}$ ($x = 0$–0.4) alloys: (a) $x = 0$; (b) $x = 0.05$; (c) $x = 0.2$; and (d) $x = 0.4$.

Table 1
Average molar fraction of elements in the alloys $(Bi_2Te_3)_{0.9}$–$(Bi_{2-x}Ag_xSe_3)_{0.1}$ ($x = 0$–0.4) analyzed by EMPA (four different points were taken when analyzed)

Samples with x element	Molar fraction of elements			
	$x = 0$	$x = 0.05$	$x = 0.2$	$x = 0.4$
Ag		0	0.009	0.036
Se	0.283	0.278	0.281	0.279
Te	2.648	2.669	2.654	2.662
Bi	1.983	1.979	1.973	1.958
Remaining elements	Oxygen			

cannot quantitatively identify the existence of possibly formed trace of Ag_2Se, which can be assumed to be preferentially precipitated due to its higher melting point (890 °C) than those of Bi_2Te_3 (586 °C) and Bi_2Se_3 (705 °C). This was actually confirmed through XRD analysis due to no obvious Ag-related phases detected in all the alloys and most main peaks for the samples show almost the same intensities. Although other Ag-related compounds such as Ag–Te alloys can be expected to form while melting, these are not identified in the XRD patterns either. Table 1 shows the average molar fraction of elements in the $(Bi_2Te_3)_{0.9}$–$(Bi_{2-x}Ag_xSe_3)_{0.1}$ alloys analyzed by EPMA, for the sample with molar fraction $x = 0.05$ we did not obtain trace of Ag element, only very limited Ag content with molar fraction of 0.009 was detected for the sample with molar fraction $x = 0.2$. In Table 1, one can easily find the average Ag content analyzed increases gradually with molar fraction x, but the distribution of elements, especially Ag, is to a certain extent inhomogeneous throughout the samples, this can be confirmed by the fact that different shots using EPMA on a sample obtain chemical compositions with some deviation from each other. In terms of these analyses, we suggest that the

samples be subjected to annealing process to make the elements distribute homogenously as much as possible. Nevertheless, the effect of small amount of Ag on the thermoelectric properties is still very important and should be taken into account here.

The relationship between Seebeck coefficients (α) and temperature is presented in Fig. 2, where the role of Ag element in the alloys is obviously played. The α values are negative for the entire temperature range, indicating n-type semiconductor behavior. With the increasing of Ag concentration the absolute α values have an increase and the maximum absolute α value is 181 (μV/K) at 409 K for the sample with $x = 0.4$, while that of $(Bi_2Te_3)_{0.9}$–$(Bi_2Se_3)_{0.1}$ is only 155 (μV/K). These results also confirm the previous assumption that the element Ag substitution for Bi behaves donor action in the $(Bi_2Te_3)_{0.9}$–$(Bi_{2-x}Ag_xSe_3)_{0.1}$ alloys, and implying that the substitution of Ag atom for Bi in the Bi_2Se_3 can result in a possible decrease both in the concentration of free electrons and mobility. This suggestion is in agreement with that reported by P. Lošt'ák et al. [14,15] who found that an incorporation of the Sb (In) atoms into the Bi_2Se_3 crystal lattice qualitatively changes the concentrations of point defects in the $(Bi_{1-x}Sb_x)_2Se_3$ and $(Bi_{1-x}In_x)_2Se_3$ crystals, presuming that the substitution of Bi by Sb (In) atoms results in a decrease in the concentration of Se vacancies V''_{Se} and antisite defects Bi'_{Se}, resulting in a suppression of free electron concentration and mobility in the range of a high Sb (In) content. The same results were also demonstrated in Ref. [16] that an increase of As concentration can help to suppress the enhancement of concentration of free electrons in the $Bi_{2-x}As_xSe_3$, but the mobility reported there increases at the same time. With an increase of temperature in the present work the α values increase until reaching the maximum at each specific x value and then decrease. The temperature at which the maximum α values appear is around 410 K.

The temperature dependence of electrical conductivity (σ) is plotted in Fig. 3, where one can find that the electrical conductivity decreases with Ag concentration, the higher Ag concentration in the $(Bi_2Te_3)_{0.9}$–$(Bi_{2-x}Ag_xSe_3)_{0.1}$ alloys, the lower the electrical conductivities. In the present samples, the composition of Bi_2Te_3 is fixed with the molar fraction 0.9, therefore the key point for the explanation of the variation of electrical conductivity should be focused on the mechanism of different amount of Ag substitution for Bi in the $Bi_{2-x}Ag_xSe_3$ alloys. Since the σ value is directly proportional to the mobility (μ) and carrier concentration n, according to the expression $\sigma = ne\mu$, the decreased σ values result from the decrease of the concentration of free electrons, or the decrease of the mobility that is ascribed to the scattering of free carriers by acoustic phonons [16], or both. According to the Plecháček suggestion [17], the decrease of σ values is most likely due to the incorporation of Ag atoms into the crystal lattice, thus changing the formation energy of the lattice defects in the $Bi_{2-x}Ag_xSe_3$ mixed crystals. But unfortunately, we did not obtain the sufficient evidence to confirm the above assumption yet.

With the increasing temperature the σ values decrease almost linearly. Fig. 3 shows that the conductivity ratio for $x = 0$ to 0.4 increases as the temperature decrease. This is expected because ionized impurity scattering becomes relatively more important at lower temperatures and there are more impurities in the $x = 0.4$ sample.

The thermal conductivity (κ) can be written as $\kappa = \kappa_L + \kappa_{carrier}$, where κ_L and $\kappa_{carrier}$ are lattice and electronic components. The latter can roughly be calculated from experimental values of electrical conductivity (σ) using the Wiedemann–Franz relation $\kappa_{carrier} = LT\sigma$, where L is the Lorenz number ($1.5 \times 10^{-8}\,W\,\Omega\,K^{-1}$) [18] and T is

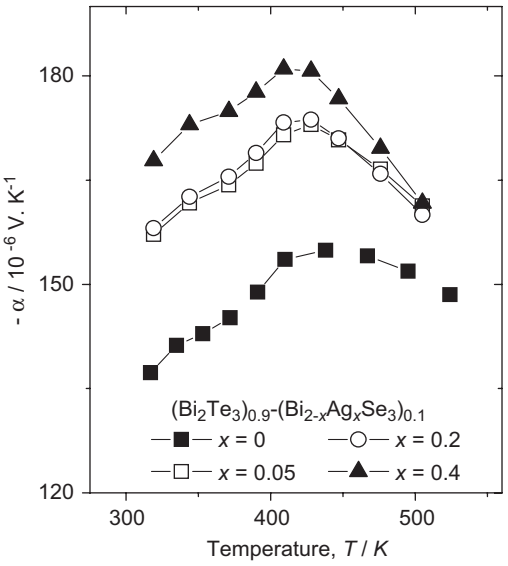

Fig. 2. The relationship between temperature and Seebeck coefficients for different $(Bi_2Te_3)_{0.9}$–$(Bi_{2-x}Ag_xSe_3)_{0.1}$ ($x = 0$–0.4) alloys prepared by spark plasma sintering.

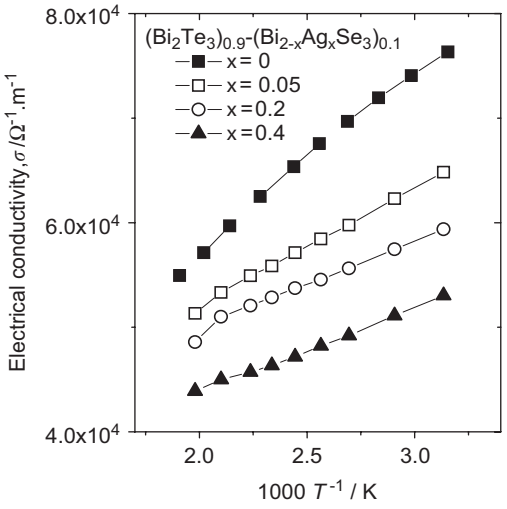

Fig. 3. The dependence of electrical conductivities on temperature for different $(Bi_2Te_3)_{0.9}$–$(Bi_{2-x}Ag_xSe_3)_{0.1}$ ($x = 0$–0.4) alloys prepared by spark plasma sintering.

the absolute temperature. The total thermal conductivities (κ) against temperature from 318 to 524 K are plotted in Fig. 4(a). Below 400 K, almost unchanged κ values ($0.96\,W\,K^{-1}\,m^{-1}$) are obtained for the alloys with $x = 0$ and 0.05. When $T > 400$ K, both these alloys show the same variation trend. However, when $x \geqslant 0.2$ an opposite variation can be observed, κ values show weak increasing tendency until the temperature reaches 400 K and then decrease. The total thermal conductivities with $x = 0.4$ are a little lower than those with $x = 0.2$. The results obtained for the temperature dependence of $\kappa_{carrier}$ are indicated in Fig. 4(b) as an inset, the $\kappa_{carrier}$ values decrease with Ag concentration, and range from 0.26 to 0.44 ($W\,K^{-1}\,m^{-1}$). With the temperature increasing the $\kappa_{carrier}$ values show mild increasing tendency. Subtracting the electronic component of thermal conductivity $\kappa_{carrier}$ from the total thermal conductivity κ we obtain the lattice thermal conductivity κ_L, shown in Fig. 4(b). It appears that, as expected, the κ_L values decrease mildly with temperature below 400 K. Above 400 K, like the variation of κ, an increase for the alloy with $x = 0$, 0.05 and a relatively rapid decrease with temperature for the alloys with $x = 0.2$, 0.4 are observed, respectively. At low contents of Ag, the phonon scattering in native defects in the pseudo-binary $(Bi_2Te_3)_{0.9}$–$(Bi_{2-x}Ag_xSe_3)_{0.1}$ alloys prevails; while at higher Ag contents, introduced point defects, the impurities and grain boundaries become dominant sources to phonon scattering and suppress the electronic as well as lattice thermal conductivity. This explanation can also partially be supported by Navrátil et al. [15] who suggested that in In-doped Bi_2Se_3 crystals phonon scattering by point defects ($In_{Bi}^{\times}$) plays an important role. Another possibility is that the apparent increase of lattice thermal conductivity above 400 K for the alloys with $x = 0$, 0.05 is attributed to ambipolar contribution arising from the diffusion of electron–hole pairs with the onset of intrinsic contribution that is apparently indicated in the α–T curves, shown in Fig. 2.

The thermoelectric figure of merit (ZT) of the pseudo-binary $(Bi_2Te_3)_{0.9}$–$(Bi_{2-x}Ag_xSe_3)_{0.1}$ ($x = 0$–0.4) alloys were calculated from the above physical properties, according to the expression, $ZT = \alpha^2\sigma/\kappa$, over the entire temperature range. The results obtained are shown in Fig. 5, where one can observe that the ZT value increases with Ag concentration, in accordance with the observed transport properties. The maximum value is about 0.86 for the alloy with $x = 0.4$ at 505 K, about 0.2 higher than that of the alloy without Ag-doping. This result is superior to that of 95% Bi_2Te_3–5% Bi_2Se_3 fabricated by gas atomizing and hot extrusion [4] and can also be comparable to that of single crystal $Bi_2(Te_{1-x}Se_x)_3$ reported in Ref. [5]. The temperature at which the maximum value appears shifts to a higher temperature for $x = 0.2$, 0.4 samples compared to $x = 0$, 0.05 ones.

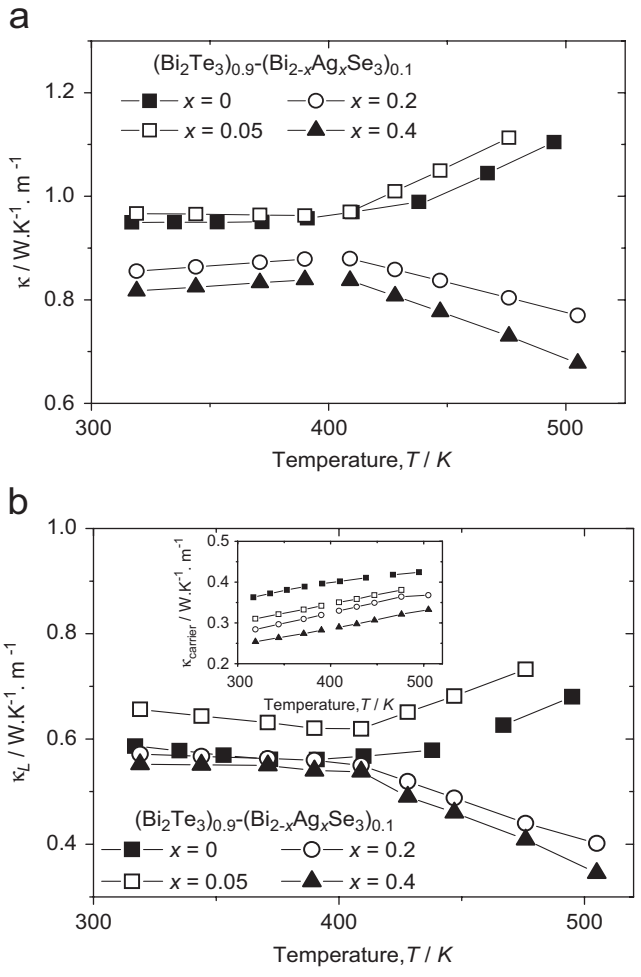

Fig. 4. The temperature dependence of thermal conductivities for different $(Bi_2Te_3)_{0.9}$–$(Bi_{2-x}Ag_xSe_3)_{0.1}$ ($x = 0$–0.4) alloys prepared by spark plasma sintering: (a) κ–T; and (b) κ_L–T (the temperature dependence of electronic components $\kappa_{carrier}$ is shown as an inset).

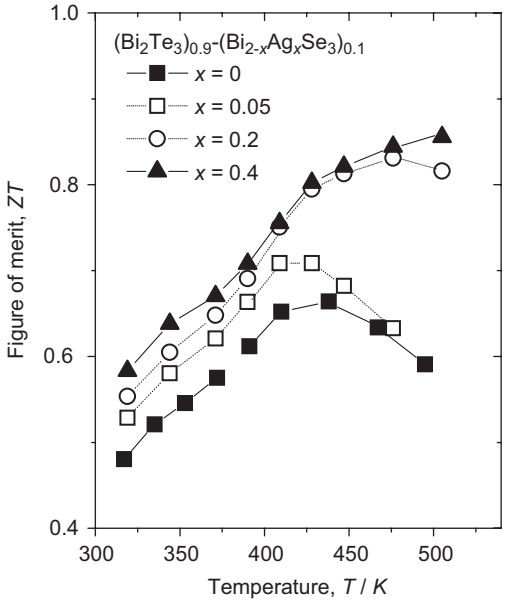

Fig. 5. The temperature dependence of dimensionless thermoelectric figure of merit ZT for different $(Bi_2Te_3)_{0.9}$–$(Bi_{2-x}Ag_xSe_3)_{0.1}$ ($x = 0$–0.4) alloys prepared by spark plasma sintering.

4. Conclusions

The materials fabricated using spark plasma sintering technique indicate that the Ag substitution for Bi can noticeably alter the physical properties of the $(Bi_2Te_3)_{0.9}$–$(Bi_{2-x}Ag_xSe_3)_{0.1}$ alloys with the enhancement of Seebeck coefficients at the expense of electrical conductivities. When at low Ag content with $x \leqslant 0.05$, the variation of the lattice thermal conductivity follows the trend of the alloy $(Bi_2Te_3)_{0.9}$–$(Bi_2Se_3)_{0.1}$ without Ag-doping; while at higher Ag content with $x \geqslant 0.2$, the lattice thermal conductivity decreases with temperature. The dimensionless figure of merit ZT increases with Ag concentration, and the maximum value is about 0.86 for the alloy with $x = 0.4$ at 505 K, about 0.2 higher than that of the alloy $(Bi_2Te_3)_{0.9}$–$(Bi_2Se_3)_{0.1}$ without Ag-doping.

Acknowledgments

The Project supported by Zhejiang Provincial Natural Science Foundation of China (No. Y404321), and Ningbo Natural Science Foundation of China (No. 2006A610058).

References

[1] S.A. Ahmed, E.M.M. Ibrahim, S.A. Saleh, App. Phys. A: Mater. Sci. Pro. 85 (2) (2006) 177–184.
[2] J. Choi, H.W. Lee, B.S. Kim, H. Park, S. Choi, S.C. Hong, S. Cho, J Magnet. Magnet. Mater. 304 (1) (2006) e164–e166.
[3] S.J. Hong, B.S. Chun, Mater. Res. Bull. 38 (4) (2003) 599–608.
[4] S.J. Hong, S.H. Lee, B.S. Chun, Mater. Sci. Eng. B 98 (3) (2003) 232–238.
[5] M. Carle, P. Pierret, C. Lahalle-gravier, S. Scherrer, H. Scherrer, J Phys. Chem. Solids 56 (2) (1995) 201–209.
[6] A. Saji, S. Ampili, S.H. Yang, K.J. Ku, M. Elizabeth, J Phys. Condens. Matter 17 (19) (2005) 2873–2888.
[7] S. Urazhdin, D. Bilc, S.D. Mahanti, S.H. Tessmer, Phys. Rev. B 69 (1–7) (2004) 085313.
[8] H. Ghoumari Bouanani, D. Eddike, B. Liautara, G. Brun, Mater. Res. Bull. 31 (2) (1996) 177–187.
[9] S. Urazhdin, D. Bilc, S.H. Tessmer, S.D. Mahandi, Phys. Rev. B 66 (1–7) (2002) 161306(R).
[10] J.L. Cui, H.F. Xue, W.J. Xiu, J. Solid State Chem. 179 (2006) 3712–3716.
[11] J.L. Cui, X.B. Xu, Mater. Lett. 59 (26) (2005) 3205–3208.
[12] J.L. Cui, H.F. Xue, W.J. Xiu, Mater. Lett. 60 (2006) 3669–3672.
[13] M. Saxena, Bull. Mater. Sci. 27 (6) (2004) 543–546.
[14] P. Lošťák, Č. Daršar, H. Süssmann, P. Reinshaus, R. Novotnỳ, I. Beneš, J. Cryst. Growth 179 (1997) 144–152.
[15] J. Navrátil, T. Plecháček, J. Horák, S. Karamazov, P. Lošťák, J.S. Dyck, W. Chen, C. Uher, J. Solid State Chem. 160 (2001) 474–481.
[16] A. Sklenár, C. Darsar, A. Krejcová, P. Losták, Cryst. Res. Tech. 35 (2000) 1069–1076.
[17] T. Plecháček, J. Navrátil, J. Horák, J Solid State Chem. 165 (2002) 35–41.
[18] R. Venkatasubramanian, E. Siivola, T. Colpitts, B. O'Quinn, Nature 413 (2001) 597–602.